Inelastic Deuteron Scattering and (d,p) Reactions from Isotopes of Ti. I. $Ti^{50}(d,p)Ti^{51}$†

P. D. BARNES AND C. K. BOCKELMAN
Yale University, New Haven, Connecticut

AND

OLE HANSEN
Institute for Theoretical Physics, University of Copenhagen, Copenhagen, Denmark

AND

A. SPERDUTO
Massachusetts Institute of Technology, Cambridge, Massachusetts

(Received 11 June 1964)

The reaction $Ti^{50}(d,p)Ti^{51}$ has been investigated at 6-MeV bombarding energy. The proton spectra were recorded simultaneously at 24 scattering angles with an energy resolution of 15 keV in the multigap heavy-particle spectrograph of Enge and Buechner. Values of the transferred neutron angular momenta and of the statistically weighted spectroscopic factors for 20 levels in Ti^{51} were derived from the measurements by a zero-range distorted-wave Born-approximation analysis. Deuteron optical-model parameters for this analysis were determined by elastic scattering experiments. The results are discussed briefly in terms of the shell model with residual interactions.

I. INTRODUCTION

THE nuclear coupling schemes relevant for low-lying levels in the $f_{7/2}$-shell isotopes have been discussed from both particle[1] and collective[2] points of view. These two aspects of nuclear structure have been investigated in the present series of experiments by populating levels of titanium isotopes through a reaction which emphasizes the single-particle features of the nuclear states [the (d,p) reaction] as well as through a reaction which emphasizes the collective features [the (d,d') reaction]. Differential cross sections at 24 scattering angles of (d,p) and (d,d') reactions from isotopically separated targets of Ti^{47}, Ti^{48}, Ti^{49}, and Ti^{50} have been measured. A bombarding energy of 6 MeV was employed with an over-all energy resolution of 15 keV.

The original measurements of Pieper[3] on these nuclei have been augmented in recent years by the work of Rietjens *et al.*,[4] and, most recently, by Yntema[5,6] and by Ramavataram.[7] In the works of Refs. 5 and 6, a bombarding energy of 21 MeV was used with an energy resolution of about 250 keV. The experiments of Refs. 4 and 7 employed bombarding energies of 7.8 MeV and energy resolutions of the order of 30 keV. The higher energy resolution and the use of isotopically pure targets in the present work proved to be essential at excitation energies above 3 MeV, where the level density is of the order of 20 levels per MeV.

The present report is concerned with the reaction $Ti^{50}(d,p)Ti^{51}$. Subsequent papers will discuss the (d,p) and (d,d') reactions on the other stable titanium isotopes, except for $Ti^{46}(d,p)Ti^{47}$, which has been investigated by Rapaport *et al.*[8] The results from both (d,d') and (d,p) reactions have been analyzed by distorted-wave Born-approximation (DWBA) methods. For the (d,p) reactions the values of the transferred orbital angular momenta and the absolute strengths referred to, respectively, as l_n and $(2J_f+1)S_{lj}$, J_f being the final-state spin, have been obtained. The results will be discussed in each paper in terms of the shell model with residual interactions.

II. EXPERIMENTAL METHOD

The experimental methods and procedures were almost identical for all the targets investigated. They will be described in some detail in this section.

II.1. Targets

Targets of $Ti^{46,47,49,50}$ for the nuclear reaction measurements were prepared in the Copenhagen isotope separator by the retardation method (see, e.g., Refs. 9 and 10). Targets of $Ti^{47,48,49,50}$ used for elastic deuteron scattering measurements were produced by vacuum

† This work was supported in part by the U. S. Atomic Energy Commission under contracts AT (30-1)2098 and AT (30-1)2627.

[1] A. de-Shalit, in *Selected Topics in Nuclear Theory*, edited by F. Janouch (I.A.E.A., 1963); J. D. McCullen, B. F. Bayman, and L. Zamick, Phys. Rev. **134**, B515 (1964).

[2] G. Scharff-Goldhaber and J. Weneser, Phys. Rev. **98**, 212 (1955); B. J. Raz, *ibid.* **114**, 1116 (1959); **129**, 2622 (1963); R. D. Lawson, *ibid.* **124**, 1500 (1961); R. D. Lawson and B. Zeidman, *ibid.* **128**, 821 (1962).

[3] G. F. Pieper, Phys. Rev. **88**, 1299 (1952).

[4] L. H. Rietjens, O. M. Bilaniuk, and M. H. Macfarlane, Phys. Rev. **120**, 527 (1960).

[5] J. L. Yntema, Phys. Rev. **127**, 1659 (1962).

[6] J. L. Yntema, Phys. Rev. **131**, 811 (1963).

[7] K. Ramavataram, Phys. Rev. **132**, 2255 (1963).

[8] J. Rapaport, Ph.D. thesis, Massachusetts Institute of Technology, 1963 (unpublished).

[9] G. Sidenius and O. Skilbreid, in *Electromagnetic Separation of Radioactive Isotopes* (Springer-Verlag, Vienna, 1961), pp. 234, 243.

[10] J. H. Bjerregaard, P. F. Dahl, O. Hansen, and G. Sidenius, Nucl. Phys. **51**, 641 (1964).

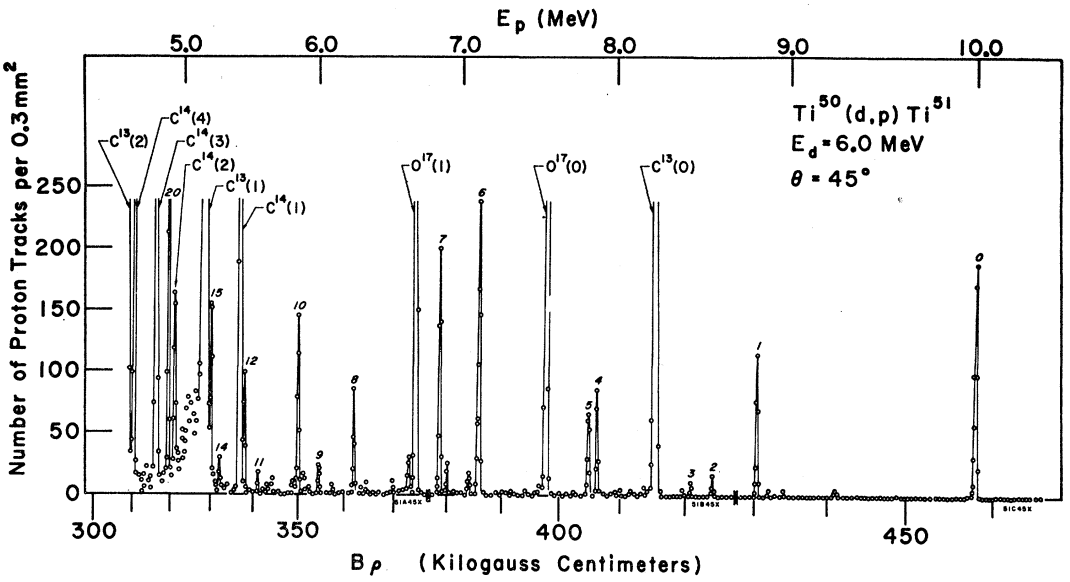

FIG. 1. Measured proton spectrum at laboratory angle 45°. The number of proton tracks in a 0.5-mm strip across the exposed zone is plotted against position along the photographic emulsion. The spectrograph calibration fixes the superimposed scale of magnetic rigidity. Proton groups identified by their kinematic shift as arising from levels in Ti^{51} are labeled with the numbers used to identify these states in Table III. Prominent contaminant groups arising from carbon and oxygen are also identified.

evaporation of TiO_2 enriched in the relevant isotope obtained from Oak Ridge National Laboratory, Stable Isotopes Division. An evaporated target of Ti^{48} was used for the nuclear reaction study. Thicknesses were approximately 30 $\mu g/cm^2$ for the separated targets and 50 $\mu g/cm^2$ for the evaporated ones; carbon foils were employed as backings. The main impurities were C^{12}, C^{13}, N^{14}, and O^{16} (from the backings), and traces of Si^{28} and S^{32}. The evaporated targets also contained Ta^{181}. The isotopic composition of each target is given in Table I. In addition, a measurement of the absolute reaction cross sections employed a target evaporated from natural titanium metal.

II.2. Elastic Scattering Measurements

Angular distributions of elastically scattered deuterons were measured in order to provide information on the optical-model parameters to be used in the DWBA computations and in order to establish an absolute cross-section scale.

The measurements were performed partly at the Copenhagen 6-MV tandem electrostatic generator and partly at the Copenhagen 4-MV electrostatic generator. In both cases the scattered particles were detected by semiconductor counters and registered in a 512-channel pulse-height analyzer. As stated above, the targets used in the (d,d) experiments contained a fair amount of Ta, and the numbers derived from the measurements were the ratio of the yield of Ti to the yield of Ta, a number that is assumed to be proportional to $d\sigma_{el}/d\sigma_{Rutherford}$. This method was chosen in order to make the results depend as little as possible on beam integrator calibrations and dead time losses.

The tandem experiment consisted in the measurement of an angular distribution at 6.00 MeV and of an excitation function at 75° scattering angle from 6 to 3.50 MeV plus a measurement at 45°, 3.50 MeV. This program was carried out for all four target nuclei.

The 4-MV experiments were made on Ti^{47} and Ti^{48} only. In the Ti^{47} case, angular distributions at 4.00, 3.50, 3.00, and 2.50 MeV were taken together with excitation functions at 60°, 90°, and 135°. In the Ti^{48} case, only one excitation function (90°) was taken. At 2.50 MeV, the yield ratio of Ti to Ta was constant. We therefore conclude that the elastic deuteron scattering from Ti at 2.50 MeV is Rutherford scattering. At 3.50 MeV, the cross sections for Ti^{47} and Ti^{48} follow the Rutherford formula at forward angles inside ±5%; it was assumed that the Ti^{49} and Ti^{50} elastic cross sections at 3.50 MeV and 45° equal the Ti^{47} and Ti^{48} cross sections.

TABLE I. Isotopic composition of the targets.

Experiment	Percentage abundances				
	Ti^{46}	Ti^{47}	Ti^{48}	Ti^{49}	Ti^{50}
$Ti^{47}(d,p)$; (d,d')		>99	<1		
$Ti^{47}(d,d)$	1.7	82.7	13.8	1.0	0.8
$Ti^{48}(d,p)$; (d,d'); (d,d)	0.2	0.2	99.3	0.2	0.1
$Ti^{49}(d,p)$; (d,d')			<1	>99	
$Ti^{49}(d,d)$	1.3	1.3	14.5	81.5	1.4
$Ti^{50}(d,p)$; (d,d')				<0.5	>99
$Ti^{50}(d,d)$	1.5	1.6	11.9	3.5	81.5

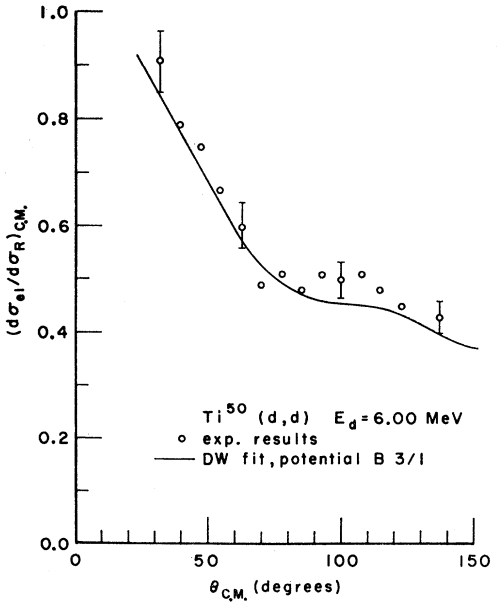

FIG. 2. Angular distribution of deuterons scattered elastically by Ti^{50} at 6 MeV. Open circles represent experimental data, and the curve is the optical-model best fit (d potential B 3/1). The fit obtained from the average potential $B4$ is equally good, whereas the PB1 potential gives a poorer fit.

In accordance with this, the Ti^{47} and Ti^{48} 6- to 3.50-MeV excitation functions were matched to the corresponding 4-MV data, the absolute normalization being based on the assumption that the 2.50-MeV cross section is equal to the Rutherford cross section. The Ti^{47} and Ti^{50} excitation functions were normalized at 3.50 MeV and 45° to 95% of the Rutherford cross section, the average of the Ti^{47} and Ti^{48} data.

In all cases the statistical accuracy was better than 5%.

From several checks on the reproducibility of these data, we assign a relative error to the angular distribution data of 5% and an absolute error of 8% to all data. Accumulating the errors involved in the normalization procedure we arrive at an error of ±22% on the absolute cross-section scale.

II.3. Nuclear Reaction Experiments

The measurements of the (d,p) and the (d,d') angular distributions were performed at the Massachusetts Institute of Technology. The isotopically separated targets were exposed to a 6.00-MeV deuteron beam from the MIT-ONR electrostatic generator and the reaction products were detected on photographic plates in the 24-gap heavy-particle spectrograph of Enge and Buechner.[11] The exposures typically were 3500 μC.

In the bombardments of Ti^{50} and Ti^{48} the 50 μ Eastman NTA photographic emulsions were covered by an Al foil of thickness such that only protons were recorded. In the Ti^{47} and Ti^{49} cases, protons, deuterons, tritons, and α particles from the respective deuteron-induced reactions were recorded simultaneously. The plates were scanned selectively for the different tracks which differed enough in length and density to be clearly distinguished from each other. The number of α and t tracks was too low to allow the extraction of useful information on the (d,t) and (d,α) reactions on Ti.

The resulting energy resolution for proton and deuteron groups was approximately 15 keV. A typical (d,p) spectrum from Ti^{50} is shown in Fig. 1.

Absolute Q values for four low-lying levels in Ti^{51} were obtained from additional measurements in the MIT single-gap spectrograph. The single-gap values agreed with the values of Ref. 10, while numbers from the 24-gap instrument were shifted systematically towards lower values. At the time the Ti^{51} angular distributions were performed, it was not possible to cycle the iron of the 24-gap spectrograph; as a result of differential hysteresis phenomena it proved difficult to establish a Q-value scale using the same magnetic field for all gaps. It was found, however, that the application of an effective field for each gap could remedy this defect. The magnitudes of these fields were obtained by demanding that four low-lying Ti^{51} groups have Q values as measured in the single-gap spectrograph. The resulting effective fields differed from the nominal value by less that 0.1% in the worst case; the average deviation was 0.03%. The original relation between distance

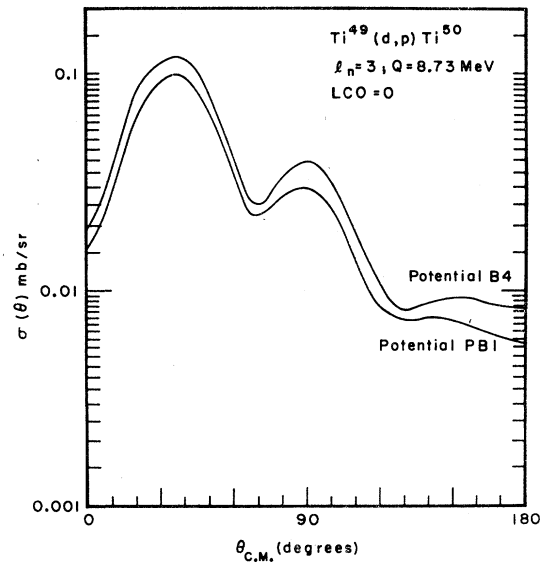

FIG. 3. DWBA predictions of (d,p) angular distributions from Ti^{49}, Q=8.73 MeV and l_n=3. The two curves were generated by potentials $B4$ and PB1, respectively. The calculated numbers $\sigma(\theta)$ are related to the experimental differential (d,p) cross section by Eq. (3). The total (d,p) cross section predicted by potential $B4$ is about 20% higher than that predicted by the PB1 potential. The $B4$ potential has been used in deriving the strengths from the experimental distributions.

[11] H. A. Enge and W. W. Buechner, Rev. Sci. Instr. 34, 155 (1963).

TABLE II. Optical-model parameters used in the (d,p) analysis.[a]

Particle	Potential	Ident. mark	V (MeV)	W' (MeV)	r_0	a	r_0' (F)	a'	r_{0c}
d	Best fit $Ti^{47}(dd)$	$B3/1$	41	19.6					
d	Best fit $Ti^{48}(dd)$	$B3/1$	99	28.2					
d	Best fit $Ti^{49}(dd)$	$B3/1$	95	29.5	1.00	0.90	1.41	0.65	1.30
d	Best fit $Ti^{50}(dd)$	$B3/1$	106	21.2					
d	Average $Ti^{48,49,50}$	$B4$	103	25.0					
d	B-type Perey[b]	PB1	92	31.2	1.15	0.81	1.34	0.68	1.30
p	Extrapolation[c]	···	52	12.0	1.25	0.65	1.25	0.47	1.25

[a] The first column identifies the particle (proton or deuteron) to which the potential applies; the second column shows how the potential was obtained; in the third column is a label used to identify the parameter set from which the calculated angular distributions were generated. The remaining columns give the values of the parameters in formula (1) for each potential used in the (d,p) analysis.
[b] C. M. Perey and F. G. Perey, Phys. Rev. 132, 755 (1963).
[c] Extrapolated from fits to data at higher energies.

along the plate and "radius of curvature" as found from calibrations with a Po^{210} α source was retained. Agreement of the Q values of easily recognizable impurity groups with values given in the literature guaranteed that systematic errors introduced by this procedure were not significant.

The effective fields were used for identification of the mass associated with each particle group by observation of the change of particle energy with angle. In addition, the effective fields furnish a scale of Q values for the titanium levels. We have adopted the absolute values from the single-gap measurements together with Q-value differences from the 24-gap runs when constructing level schemes. The absolute Q value for the Ti^{51} ground-state transition was measured as 4.151 $\pm$0.006 MeV, based on an energy standard for Po^{210} α particles of 5.3042$\pm$0.0016 MeV.

The cross section scale in the 24-gap experiments was established by observing the ratio of elastic scattering to (d,p) yield from a target of natural titanium for several strong proton groups from each of the isotopes. The elastically scattered deuterons were recorded immediately before and after the nuclear reaction experiment, by taking exposures on each of the adjacent zones on the plates (see Ref. 11). By this means a cross section scale for the (d,p) reaction was obtained relative to the elastic scattering of 6-MeV deuterons from titanium of normal isotopic constitution. An error of 10% is assigned to these measurements. The elastically scattered deuteron yield was then normalized to the elastic scattering results described in Sec. II.2. The absolute (d,p) cross sections thus depend on the elastic scattering results of Sec. II.2; but the relative cross sections for the four Ti isotopes do not. We assign an error of 24% on the absolute cross sections (cf. the discussion in Sec. II.2).

In cases where impurity proton groups partly obscure proton groups from Ti, corrections were applied, using experimental distributions from the literature.[12] The statistical accuracy of individual points of the (d,p) distributions vary from 2% in the most favorable cases to 10% in the worst cases.

III. RESULTS AND ANALYSIS

The first subsection includes to a description of the optical-model analysis of the 6-MeV (d,d) distributions. In the second subsection the $Ti^{50}(d,p)Ti^{51}$ results are presented.

III.1. Optical Model and DWBA Analysis

A typical example of an elastic deuteron distribution is given in Fig. 2, which shows the $Ti^{50}(d,d)$ results (open circles) together with the optical-model fit (full drawn curve).

Each of the four 6-MeV distributions were analyzed[13]

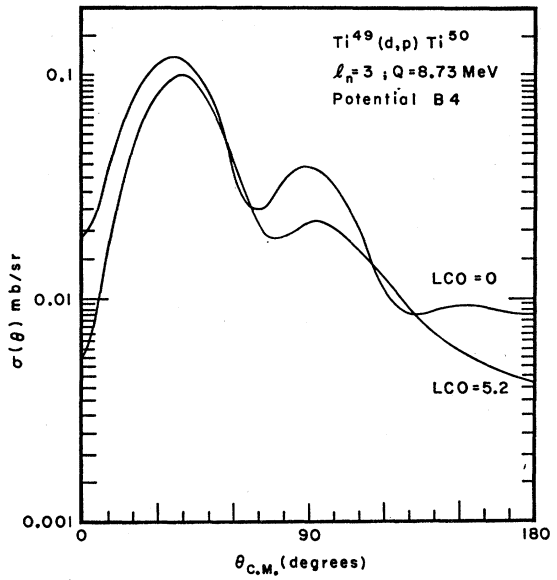

FIG. 4. Influence of lower cutoff radius on predicted distributions. The present example provides the largest effect observed in these calculations. At lower Q values the influence of the lower cutoff radius is barely perceptible.

[12] We wish to thank Dr. J. Janecke for communicating his results on the $S^{32}(d,p)S^{33}$ reaction before publication.

[13] The optical-model analysis was performed by Dr. G. R. Satchler at the Oak Ridge National Laboratory.

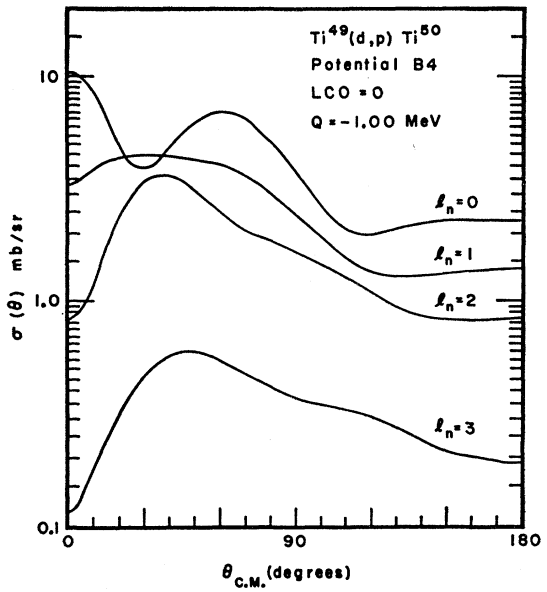

FIG. 5. DWBA predictions for $Ti^{49}(d,p)Ti^{50}$, $Q=-1.00$ MeV and l_n values from 0 to 3. For the definition of $\sigma(\theta)$ see Sec. III.2, Eq. (3). This figure shows that even at low Q values the calculated angular distributions of different l_n values are easily distinguished from each other.

by an optical potential of the form

$$U(r)=-\frac{V}{1+\exp x}+4iW'\frac{d}{dx'}\left(\frac{1}{1+\exp x'}\right)+V_c(r,r_c), \quad (1)$$

where

$$x=(r-r_0A^{1/3})/a,\ x'=(r-r_0'A^{1/3})/a', \text{ and } r_c=r_{0c}A^{1/3}.$$

V and W' designate the magnitudes of the real and absorptive potentials, respectively; V_c is the Coulomb potential from a homogeneously charged sphere of radius r_c. The parameters were sought by varying V and W' while keeping a, a', r_0, r_0', and r_{0c} fixed; fits were obtained for a number of sets of (a, a', r_0, r_0', r_{0c}) values. The resulting best-fit values of all parameters are given in Table II for each of the four Ti isotopes. The best fits did not deviate by more than 10% from experiment in any case.

The $Ti^{48,49,50}$ distributions resemble each other closely; it was possible to fit them with deviations no greater than $\simeq$10% with a single potential. The parameters of this average potential are also listed in Table II. A sixth potential using different values for a, a', r_0, and r_0' was also employed; it afforded a test of the sensitivity of the DWBA calculations to variation of the parameters of the deuteron potential. The parameters of the complex potential for the outgoing proton were extrapolated from fits to data at higher bombarding energies.[13] The values used in the calculation of the (d,p) distributions are also given in Table II.

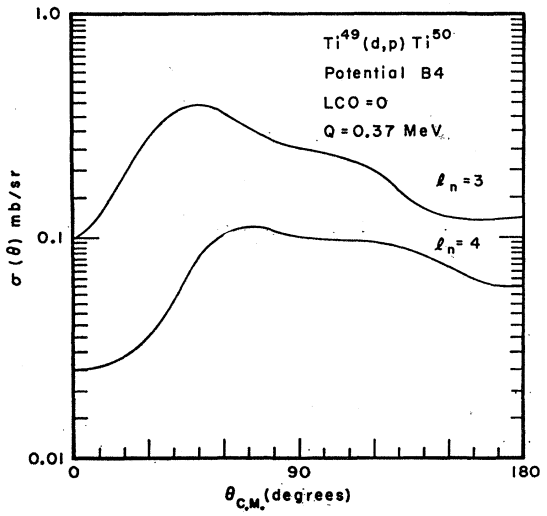

FIG. 6. DWBA predictions for $Ti^{49}(d,p)Ti^{50}$, $Q=0.37$ MeV and $l_n=3$ and 4. See also the caption of Fig. 5.

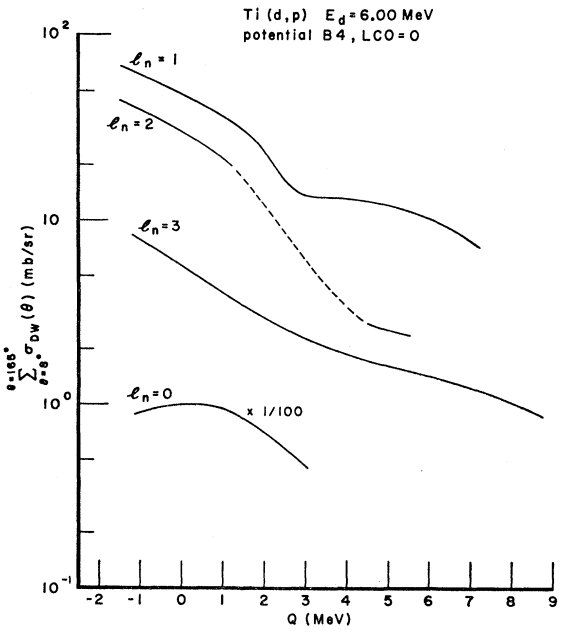

FIG. 7. Q and l_n dependence of $\sigma(\theta)$ as obtained from DWBA theory. The curves shown correspond to the sum $\Sigma\,\sigma(\theta)$ over the first twenty-two angles at which the (d,p) angular distributions were measured (from 7.5 to 165° in steps of 7.5° in the laboratory system). In deriving the $(2J_f+1)S_{lj}$ from measurements, the above curves were used for interpolation in Q.

From the potentials of Table II angular distributions $\sigma(\theta)$ were predicted for the (d,p) reactions. The captured neutron in the final state was described as moving in a Saxon well. The calculations were zero-range calculations[14] and a lower cutoff (abbreviated LCO) could be used on the radial integrals. The effects on the calcu-

[14] R. H. Bassel, R. M. Drisko, and G. R. Satchler, ORNL 3240 (Office of Technical Services, Department of Commerce, Washington); G. R. Satchler, Nucl. Phys. 55, 1 (1964).

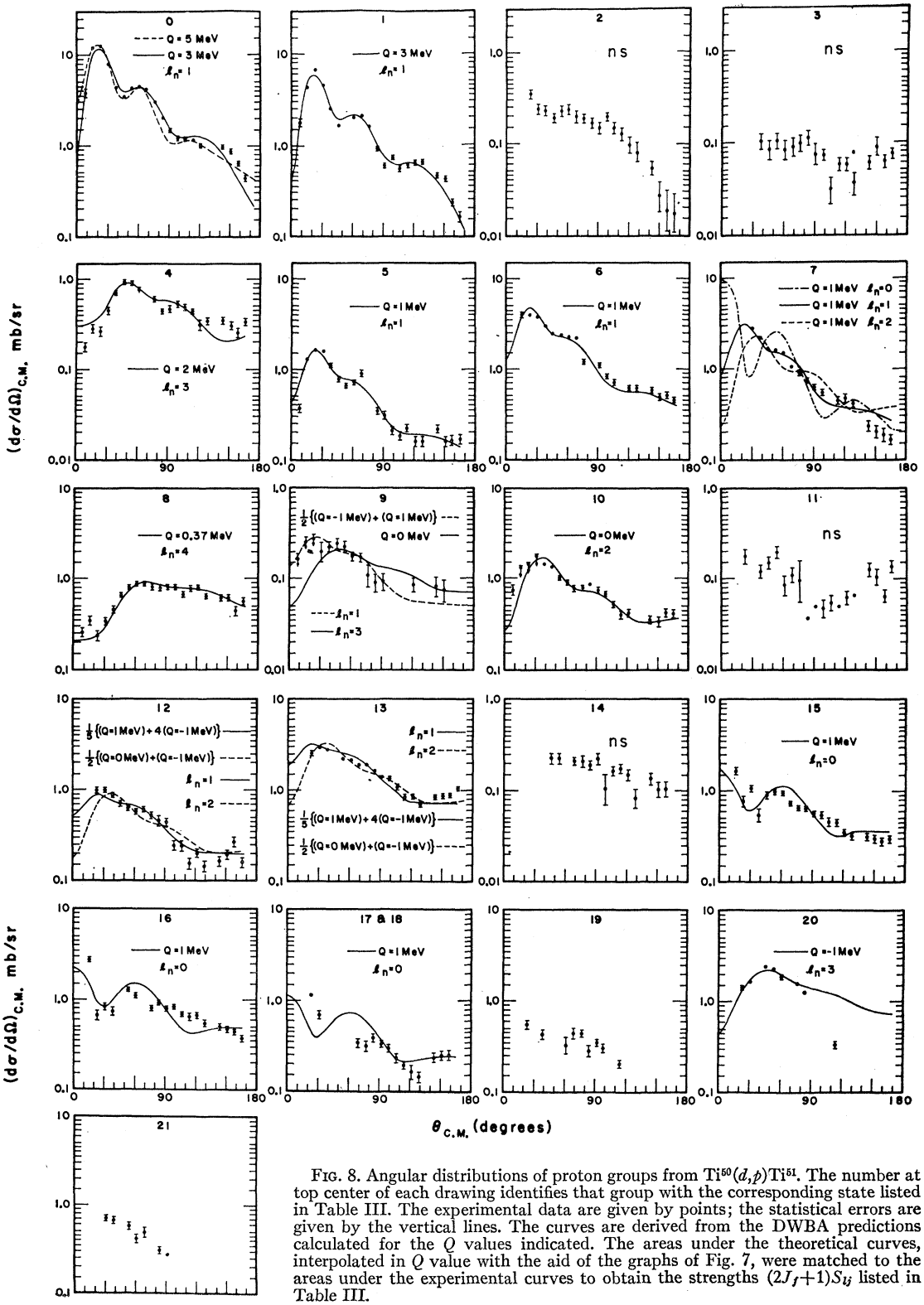

FIG. 8. Angular distributions of proton groups from $Ti^{50}(d,p)Ti^{51}$. The number at top center of each drawing identifies that group with the corresponding state listed in Table III. The experimental data are given by points; the statistical errors are given by the vertical lines. The curves are derived from the DWBA predictions calculated for the Q values indicated. The areas under the theoretical curves, interpolated in Q value with the aid of the graphs of Fig. 7, were matched to the areas under the experimental curves to obtain the strengths $(2J_f+1)S_{lj}$ listed in Table III.

TABLE III. $Ti^{50}(d,p)Ti^{51}$ results.[a]

Level No.	E (MeV)	l_n	$J_f\pi$	$(2J_f+1)S_{lj}$
0	0	1	$\frac{3}{2}-$	3.65±0.35
1	1.160	1	$\frac{5}{2}, \frac{1}{2}-$	1.71±0.15
2	1.429	n.s.	...	...
3	1.559	n.s.	...	...
4	2.136	3	$\frac{5}{2}-$	2.36±0.25
5	2.189	1	$\frac{3}{2}, \frac{1}{2}-$	0.34±0.04
6	2.896	1	$\frac{3}{2}, \frac{1}{2}-$	0.73±0.07
7	3.164	1	$\frac{3}{2}, \frac{1}{2}-$	0.41±0.04
8	3.759	4	$\frac{9}{2}+$	5.39±0.55
9	4.012	3(1)	$\frac{5}{2}-$	0.34±0.04
10	4.162	2	$\frac{5}{2}+$	0.36±0.04
11	4.460	n.s.	...	...
12	4.559	1	$\frac{3}{2}, \frac{1}{2}-$	0.12±0.02
13	4.592	2	$\frac{5}{2}+$	0.65±0.07
14	4.747	n.s.	...	...
15	4.810	0	$\frac{1}{2}+$	0.11±0.02
16	4.872	0	$\frac{1}{2}+$	0.15±0.02
17	4.988	(0)	$\frac{1}{2}+$	0.10±0.02
18	5.003			
19	5.092	?	...	...
20	5.139	3	$\frac{5}{2}-$	2.41±0.25
21	5.214	?	...	...

[a] Column 2 gives the excitation energies obtained according to the discussion in Sec. II.3. The error in all cases is ±10 keV. The Q value of the ground-state group is 4.151±0.006 MeV. The observed l_n values are given in column 3. The next column lists the final state spins and parities, ascribed as discussed in the text. The last column shows the strengths $(2J_f+1)S_{lj}$. The errors on the strengths are statistical and scanning errors, only. The uncertainty in the magnitude of the absolute cross section is ±24%.

lated (d,p) distributions of varying the deuteron potential (Fig. 3) or the lower cutoff radius (Fig. 4) were not large. The l_n values and the S_{lj} given in the next subsection were obtained from a series of DWBA predictions which used the $Ti^{48,49,50}$ average potential ($E4$) and a LCO radius of 0. The effect of the variation in target mass among the separate Ti isotopes was small; to minimize the number of calculations required, a target mass of 49 was used in all cases. These predictions always represent an acceptable fit to the experimental distributions as evidenced by Fig. 8 of Sec. III.2. The calculations were performed for several Q values between −1 and +8.7 MeV for l_n values between 0 and 4. Figures 5 and 6 demonstrate that the predicted distributions for $l_n=0$, 1, 2, and 3 (Fig. 5) and $l_n=3$ and 4 (Fig. 6) are easily distinguished from each other, thus making l_n assignments unambiguous, except for a few cases where the data are poor.

The predicted variation of $\sigma(\theta)$ summed over angles with Q and l_n is shown in Fig. 7. In order to allow interpolations, a smooth curve was drawn connecting the calculated points. The graphs deviate in detail from the simple rule

$$\sigma(\theta) \propto 2^{-kl_n}K^{-Q} \qquad (2)$$

used by Cohen *et al.*[15]

The DWBA predictions of (d,d') angular distributions will be discussed in a separate paper.

[15] B. L. Cohen and R. E. Price, Phys. Rev. **121**, 1441 (1961); B. L. Cohen, R. E. Price, and S. Mayo, Nucl. Phys. **20**, 370 (1960).

III.2. $Ti^{50}(d,p)Ti^{51}$ Results

The angular distributions obtained for the $Ti^{50}(d,p)Ti^{51}$ reaction are shown in Fig. 8. The points represent the experimental data, and the curves are the DWBA predictions, normalized to the areas of the experimental distributions. The relation between the experimental cross sections $d\sigma/d\Omega$ and the DWBA results $\sigma(\theta)$ is given by

$$d\sigma/d\Omega=1.5[(2J_f+1)/(2J_i+1)]S_{lj}\sigma(\theta). \qquad (3)$$

Here, J_i and J_f are the initial and final nuclear spins, respectively; the numerical factor 1.5 is associated with the use of the Hulthén wave function to describe the deuteron. Thus the area normalization directly yields the transition strength $(2J_f+1)S_{lj}$, where S_{lj} is the spectroscopic factor. In Table III we have collected the values of excitation energy (E), l_n, and $(2J_f+1)S_{lj}$ as obtained in the present experiment. For a number of cases Table III also proposes a value of J_f, namely when the shell model furnishes a reason to prefer one of the values of $l_n\pm\frac{1}{2}$ over the other; in particular, the systematics of single-neutron states as given by Cohen *et al.*[16] have been used. The main ambiguity is found in the excited $l_n=1$ states, where the closeness of the $2p_{3/2}$ and $2p_{1/2}$ orbits makes a choice arbitrary. The $l_n=1$ ground state most probably is $\frac{3}{2}-$ (see, e.g., Ref. 17).

The errors quoted on $(2J_f+1)S_{lj}$ are the statistical errors in determining the experimental areas. The errors from the uncertainty in absolute scale and the possible errors from the approximate character of the DWBA analysis are not included.

In most cases of stripping distributions it has been possible to account for the observations using one value of l_n (see Fig. 8). For levels 12 and 13 the choice between $l_n=1$ and $l_n=2$ is somewhat difficult because of the lack of data for $\theta=7.5$ and 15.0°. Nonstripping distributions are marked "n.s." in Table III under the heading "l_n". In the cases of levels 19 and 21 the experimental data are too poor to allow an l_n determination.

IV. DISCUSSION

IV.1. Levels with Stripping Character

The distribution of the statistically weighted spectroscopic factors, hereafter called the Ti^{51} strength function, is shown in Fig. 9. It is seen that strong fluctuations occur, and in particular that the strength of the p levels is spread over at least 4.5 MeV. This spread demonstrates the existence of residual interactions, for in the pure shell model the closed shell of 28 neutrons would indicate that, among the low states of Ti^{51}, only two single-neutron p states should be observed.

[16] B. L. Cohen, R. H. Fulmer, A. L. McCarthy, and P. Mukherjee, Rev. Mod. Phys. **35**, 332 (1963).

[17] Landolt-Börnstein, *Zahlenwerte und Funktionen, Neue Serie 1/1* (Springer-Verlag, Berlin, 1961).

TABLE IV. Sum-rule analysis.[a]

Strength sum	$\Sigma_a(2J_f+1)S_{lj}{}^a$ $l_n=0$ $J_f=\frac{1}{2}$	$l_n=1$ $J_f=\frac{1}{2}+J_f=\frac{3}{2}$	$l_n=2$ $J_f=\frac{5}{2}$	$l_n=3$ $J_f=\frac{5}{2}$	$l_n=4$ $J_f=\frac{9}{2}$
Theory	2	6	6	6	10
Experiment	0.36	6.96	1.01	5.11	5.39

[a] The table gives the sum of $(2J_f+1)S_{lj}$ over levels characterized by a given l_n, j. The first row states the expectations assuming $\Sigma_a S_{lj}{}^a=1$. The second row gives the corresponding experimental values taken from Table III.

Presuming a similar spread in strength for other shell-model states, the observed distribution suggests that other $l_n=0$, 2, and 4, and probably also $l_n=3$, states have not been observed. They may lie at excitation energies higher than explored in the present experiment.

A sum-rule analysis also shows that some states have been missed. Assuming that the Ti^{50} ground state has a pure $(f_{7/2})^8$ configuration, it is expected in the shell-model picture (including residual interactions) that $\sum_a S_{lj}{}^a=1$, where the sum is over all fragments a of a given state (l,j). Summing over the observed p states (to avoid the necessity of arbitrarily choosing between $J_f=\frac{1}{2}$ and $J_f=\frac{3}{2}$) the data of Table IV give a total strength of 6.96 compared to the expected value of 6.

Considering the 24% error assigned to the absolute cross sections, it is seen that the sum rule appears to be fulfilled for the p states. Further, the spectroscopic factor of the ground state of Ti^{51} is unity within experimental error, implying a single-particle $p_{3/2}$ nature for this state. Summing over the observed states of other l_n, the numbers of Table IV show that about $\frac{5}{6}$ of the $f_{5/2}$ and $\frac{1}{2}$ of $g_{9/2}$ strength have been observed in the present measurement, whereas 15% of the $s_{1/2}$ and $d_{5/2}$ strengths has been found.

The present data may also be used to locate the unperturbed single-particle energies. Denoting by E_{lj}' the excitation energy of the single-particle states in the limit of no residual interaction, we have (Ref. 18)

$$E_{lj}'\textstyle\sum_a S_{lj}{}^a=\sum_a S_{lj}{}^a E_{lj}{}^a, \qquad (4)$$

where $E_{lj}{}^a$ are the observed excitation energies. In order

TABLE V. Unperturbed single-particle binding energies (MeV).[a]

Configuration	Present experiment	Reference 16
$p_{3/2}$	5.95	6.0
$p_{1/2}$	4.58	4.0
$f_{5/2}$	≈2.86	3.0
$g_{9/2}$	<2.64	
$d_{5/2}$	<1.9	
$s_{1/2}$	<1.5	

[a] Excitation energies of the single-particle states are calculated from the results given in Table III by use of formula (4). From these numbers neutron binding energies are obtained by subtracting them from 6.40 MeV, the binding energy of the 29th neutron in Ti^{51}.

[18] S. Yoshida, Nucl. Phys. **38**, 380 (1962).

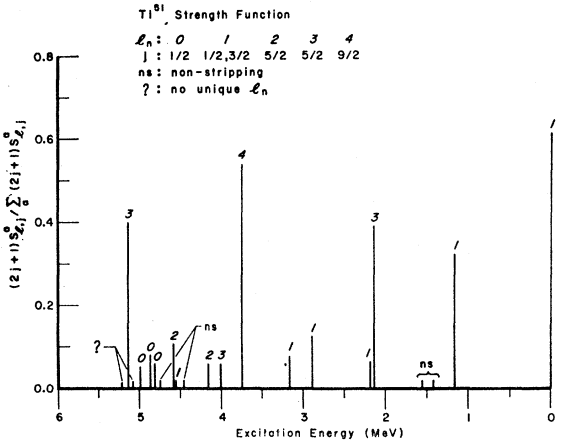

FIG. 9. Strength function for Ti^{51}. The values of $(2J_f+1)S_{lj}$ from Table III, in units of the sum-rule limits given in the first line of Table IV, are plotted against excitation energy. For all l_n other than one, a definite J_f has been assumed, as shown in the figure. For $l_n=1$, both $J_f=1\pm\frac{1}{2}$ are included in the sum-rule limit.

to apply the sum rule (4) it is necessary to know the values of J_f. Although no experimental measurements of spins exist except for the ground state, for definiteness, we have used the J_f of Table III, taking the states (0) and (6) as $J_f=\frac{3}{2}$, and states (1), (5), (7), and (12) as $J_f=\frac{1}{2}$, which choice has the advantage of fulfilling $\sum_a S_{l,1/2}{}^a=\sum_a S_{l,3/2}{}^a$. $E_{1,1/2}'$ and $E_{1,3/2}'$ are not strongly dependent on the choice of spins. The results of applying rule (4) are shown in Table V. The table shows binding energies rather than excitation energies; the 29th neutron is bound in the ground state of Ti^{51} by 6.40 MeV. The third column of Table V gives the numbers interpolated from binding energy systematics (Ref. 16). The agreement is satisfactory.

The results of Yntema on $Ti^{50}(d,t)Ti^{49}$ (Ref. 5) and of Kashy and Conlon[19] on $Ti^{50}(p,d)Ti^{49}$ seem to indicate a small admixture (5%) of p states in the Ti^{50} ground state. Consequences of such an admixture would be that the total $f_{7/2}$ strength is not used up in Ti^{50}, i.e., excited $f_{7/2}$ levels should be found in Ti^{51}, and that some of the p strength has been used in Ti^{50}, i.e., the total p strength in Ti^{51} should be less than 6. Of the three $l_n=3$ states observed here the states (4) and (20) are certainly too strong to be the $f_{7/2}$ states, whereas state (9) is not excluded by the present evidence. The detection of a decrease in p strength in Ti^{51} corresponding to the above p admixture in Ti^{50} is beyond the accuracy of the present experiment. Taking into account the difference in energy resolution, Yntema's $Ti^{50}(d,p)$ results[6] are in fair agreement with the present data. The (relative) strengths for states (0) and (1) Yntema finds as 4.8 and 2.4, respectively, compared to 3.7 and 1.7 here. The weak $l_n=3$ state inferred in Ref. 6 at 1.45 MeV presumably corresponds to the non-stripping states (2) and (3) of Table III. For higher

[19] E. Kashy and T. W. Conlon, Phys. Rev. **135**, B389 (1964).

states given in Ref. 6, the present experiment offers several candidates.

The experimental results obtained by Ramavataram[7] covering excitations to 4.6 MeV are in good over-all agreement with the numbers listed in Table III. However, states (9) and (11), which are relatively weak, appear to have been missed in the earlier experiment. Further, the use of DWBA analysis allows a fairly unambiguous assignment of $l_n=1$ to group (7) (Fig. 8), but denies the earlier assignment of $l_n=3$ given to the 1.429-MeV level. For the other states, the absolute spectroscopic factors are in quite good agreement with the relative values cited by Ramavataram using a Butler analysis together with the empirical single-particle reduced widths introduced by Macfarlane and French.[20]

The strong dip at $\theta\approx 135°$ in $l_n=1$ distributions corresponding to $p_{1/2}$ states discovered by Lee and Schiffer[21] and observed for state (1) of Ti^{51} is not seen under the present conditions (see Fig. 8).

IV.2. The Nonstripping States

Transitions of nonstripping character may be explained *ad hoc* from two points of view: (a) The l_n values are very high (in the present case at least higher than 4); (b) some selection rule makes S_{lj} small. From the general systematics of the shell model it is not very probable that the two low-lying nonstripping states at 1429 and 1559 keV would correspond to states with $l_n>4$, i.e., $h_{11/2}$ states. We therefore believe that explanation (b) is responsible for their nonstripping character. The levels in question might correspond to states involving an excited proton pair, an interpretation which is in line with the results of McCullen *et al.*[1] Interpreting the levels as being mainly of vibrational character also provides a consistent characterization. Such levels should occur at energies close to the 2+ state in the neighboring even isotopes (i.e., $\simeq$1.5 MeV). They would most probably be of nonstripping character, as vibrational levels in odd-mass nuclei are considered as built on three-particle states[22] whereas mainly one-particle states are populated by a direct (d,p) transition from an even target. This argument assumes that four-particle configurations in the even ground state may be ignored.

A vibrational description would mean that the states should be strongly populated in direct inelastic scattering. Because of the short half-life of Ti^{51} such an experiment has not been carried out. In the cases of Ti^{49} and Ti^{47} this has been done, and it is hoped that a quantitative analysis of these measurements may give information as to which of the above explanations is correct.

ACKNOWLEDGMENTS

It is a pleasure to thank G. Sidenius of the Copenhagen Isotope Separator for having prepared the targets for the nuclear reaction experiments. We are indebted to Dr. G. R. Satchler for carrying out the DWBA calculations and for providing many illuminating comments. We are particularly grateful to Professor A. Bohr and Professor B. R. Mottleson for their stimulating interest in our work. The cooperation of Professor W. Buechner and Professor H. Enge is sincerely appreciated.

The nuclear emulsions were carefully scanned by Miss Bonnie Andersen, Mrs. Ruth Hansen, Miss Birthe Klintskov, and Miss Sus Vilmann from the Copenhagen scanning group, and by Mrs. Virginia Camp, Mrs. Mieko Kitajima, and Mrs. Masako Nagatani from the Yale scanning group. The help of Mrs. Henny Bork in much of the calculation work is acknowledged.

[20] M. H. Macfarlane and J. B. French, Rev. Mod. Phys. **32**, 507 (1960).

[21] L. L. Lee and J. P. Schiffer, Phys. Rev. Letters **12**, 108 (1964).

[22] B. R. Mottelson, in *Proceedings of the International Conference on Nuclear Structure, Kingston, 1960* (University of Toronto Press, Toronto, 1960), p. 525.